

RESEARCH ARTICLE

# Lack of Spatial Subdivision for the Snapper *Lutjanus purpureus* (Lutjanidae – Perciformes) from Southwest Atlantic Based on Multi-Locus Analyses

Raimundo da Silva<sup>1</sup>✉, Iracilda Sampaio<sup>2</sup>‡, Horacio Schneider<sup>2</sup>‡, Grazielle Gomes<sup>1</sup>✉\*

**1** Laboratório de Genética Aplicada, Campus Bragança, Universidade Federal do Pará, Bragança, Pará, Brasil, **2** Laboratório de Genética e Biologia Molecular, Campus Bragança, Universidade Federal do Pará, Bragança, Pará, Brasil

✉ These authors contributed equally to this work.

‡ These authors also contributed equally to this work.

\* [graziellefeg@gmail.com](mailto:graziellefeg@gmail.com)



OPEN ACCESS

**Citation:** da Silva R, Sampaio I, Schneider H, Gomes G (2016) Lack of Spatial Subdivision for the Snapper *Lutjanus purpureus* (Lutjanidae – Perciformes) from Southwest Atlantic Based on Multi-Locus Analyses. PLoS ONE 11(8): e0161617. doi:10.1371/journal.pone.0161617

**Editor:** Michael Knapp, University of Otago, NEW ZEALAND

**Received:** March 7, 2016

**Accepted:** August 9, 2016

**Published:** August 24, 2016

**Copyright:** © 2016 da Silva et al. This is an open access article distributed under the terms of the [Creative Commons Attribution License](https://creativecommons.org/licenses/by/4.0/), which permits unrestricted use, distribution, and reproduction in any medium, provided the original author and source are credited.

**Data Availability Statement:** All data (sequences) are available in Genbank, <http://www.ncbi.nlm.nih.gov/nucleotide>. GenBank accession codes: KX448357 to KX448789, KC123167, KC122929, KC122962- KC122964, KC122981-KC122982, KC122989-KC122990, KC123050-KC123057, KC123065-KC123068, KC123071-KC123072, KC123074, KC123076, KC123078, KC123091, KC123094, KC123095, KC123097-KC123166 and KT869380-KT869392, KT869423-KT869425, KT869476-KT869485.

## Abstract

The Caribbean snapper *Lutjanus purpureus* is a marine species fish commonly found associated with rocky seabeds and is widely distributed along of Western Atlantic. Data on stock delineation and stock recognition are essential for establishing conservation measures for commercially fished species. However, few studies have investigated the population genetic structure of this economically valuable species, and previous studies (based on only a portion of the mitochondrial DNA) provide an incomplete picture. The present study used a multi-locus approach (12 segments of mitochondrial and nuclear DNA) to elucidate the levels of genetic diversity and genetic connectivity of *L. purpureus* populations and their demographic history. *L. purpureus* has high levels of genetic diversity, which probably implies in high effective population sizes values for the species. The data show that this species is genetically homogeneous throughout the geographic region analyzed, most likely as a result of dispersal during larval phase. Regarding demographic history, a historical population growth event occurred, likely due to sea level changes during the Pleistocene.

## Introduction

Due to the apparent lack of vicariant barriers in marine environments, processes leading to genetic isolation are rare compared to terrestrial continental environments [1]. In addition, inherent reproductive characteristics of many marine species (e.g., pelagic larval duration [PLD], type of egg, spawning location) have been cited as factors that promote high levels of genetic connectivity among populations [2], even those separated by large geographic distances.

The Caribbean snapper *Lutjanus purpureus* (Poey 1866) is a marine fish found in rocky and sandy seabeds, usually associated with substrate, at depths of up to 160 meters [3,4], along the Western Atlantic coast from Cuba to Southeast Brazil [3]. The species possess an external fertilization process and has a larval pelagic developmental stage [4], which may extend for

**Funding:** Funding for this research was provided by CNPq (grants 306233/2009-6 to IS, 306233/2009-6 to HS and an MSc scholarship to RS). The funders had no role in study design, data collection and analysis, decision to publish, or preparation of the manuscript.

**Competing Interests:** The authors have declared that no competing interests exist.

approximately 30 days [5]. Both of these characteristics of the reproductive strategy are likely to promote greater dispersal of individuals [1]. The Caribbean snapper has been intensely fished since half of decade of 1950 along the Brazilian coast, but few genetic studies involving *L. purpureus* have been conducted at the intraspecific level.

Previous studies of *L. purpureus* have identified high genetic diversity indices, a historical population expansion event (likely the result of sea level changes during the Pleistocene), and high levels of genetic connectivity along the Brazilian coast Gomes et al. [6,7]. However, these investigations were limited to segments of the mitochondrial control region and can therefore only provide a limited view of the genetic/population structure of this species.

The identification of processes acting on demographically independent units is fundamentally important for understanding the effects of the excessive exploitation of fish stocks [8]. Therefore, for species targeted by commercial fishing, such as *L. purpureus*, which has been fished intensively for more than half a century along the Brazilian coast, the understanding of connectivity and population history is necessary for the management purposes of stocks, implementation and success of conservation measures [8].

It is important to note that due to the stochastic nature of the coalescent process, analysis of evolutionary processes based on information contained in only one locus may not reflect the true history of the population [9] and analyses involving multiple independent loci are able to provide a more accurate view of the historical demographic processes (e.g., [10]). For example, because of differences in effective size for mitochondrial and nuclear regions, some studies using both real and simulated data, have shown that a single locus is unable of recover the demographic history occurring before a bottleneck event [10,11]. In addition, for bayesian methods of clustering of individuals, the use of multiple unlinked markers has better performance than data with few (or none) recombining regions [12].

Here we aim to analyze the genetic structure of *L. purpureus* populations to describe the historical demographic processes of the species along the Brazilian coast using a multi-locus approach (12 genomic regions—mitochondrial and nuclear DNA).

## Materials and Methods

### Ethics Statement

All the tissues used here, were obtained from dead individuals, on commercial landings in the localities mentioned above. During the sampling, *L. purpureus* was not endangered or protected along the Brazilian Coast. Therefore, there was no need to apply for a license for collection or approval by the Animal Ethics Committee. The specimens were transported with the authorization of the Brazilian Environment Ministry (permit N° 12773–1).

### Sampling

Biological samples (muscle or fin tissue) were collected between 2003 and 2010 at four locations in the Western Atlantic, in points of non-spawning and outside the reproductive period (Fig 1). All the individuals were obtained of the commercial landings in the localities. We used different landings, at each location, to ensure representativity of the stock. *L. purpureus* exemplars were identified based on specialized literature [3,13]. The collected material was stored in 96% ethanol and was frozen until laboratory processing.

### Laboratory procedures

DNA was extracted using the protocol described by Sambrook et al. [15], with adaptations for 1.5 mL tubes, or with a commercial extraction kit (Wizard Genomics—PROMEGA), following



**Fig 1. Map of the spatial distribution of *L. purpureus* specimen collection points used in this study.** CNB1- North Coast of Brazil 1 (Pará and Amapá). CNB2- North Coast of Brazil 2 (Maranhão). Map created in GMT 5.1.2 [14].

doi:10.1371/journal.pone.0161617.g001

the manufacturer's instructions. The extract was analyzed using horizontal agarose gel electrophoresis, stained with Gel Red<sup>TM</sup> (BIOTIUM) and visualized under ultraviolet light to detect the isolated material.

The genomic regions of interest were PCR-amplified using the primers described in [Table 1](#). PCRs were designed for a final volume of 15  $\mu$ L, consisting of a mixture of four deoxynucleotides (DNTPs) (200  $\mu$ M), buffer (1X), MgCl<sub>2</sub> (2 mM), 0.4  $\mu$ L of each primer (10  $\mu$ M), 0.06 U/ $\mu$ L of Taq DNA polymerase, approximately 50 ng of template DNA, and ultrapure water to complete the reaction volume. Assays without template DNA were performed to control for contamination.

Samples were sequenced by dideoxy terminator sequencing [28] in an ABI 3500 XL automatic sequencer (Applied Biosystems) using Big Dye kit reagents (ABI Prism<sup>TM</sup> Dye Terminator Cycle Sequencing Ready Reaction–Applied Biosystems, USA), following the manufacturer's recommendations. For nuclear regions, each individual was sequenced in two directions to minimize ambiguities in the identification of the sites. All the new sequences of the present study are available in Genbank under the accession codes KX448357 to KX448789.

**Table 1. Description of primers and amplification conditions for all the genomic segments used in this study.** \*- Forward primer, \*\*- Reverse primer.

Locus	Primer	Reference	Sequence 5'-3'	Annealing
CR	A*	[16]	TTCCACCTCTAACTCCCAAAGCTAG	57°C
CR	G**	[16]	CGTCGGATCCCATCTTCAGTGTATGCTT	57°C
CytB	FishCytbF*	[17]	ACCACCGTTGTTATTCAACTACAAGAAC	54°C
CytB	TrucCytbR**	[17]	CCGACTTCCGGATTACAAGACCG	54°C
ND4	ND4LB*	[18]	CAAAACCTTAATCTYCTACAATGCT	56°C
ND4	NAP2**	[19]	TGGAGCTTCTACGTGRGCTTT	56°C
S7	S7RPEX1F*	[20]	TGGCCTCTTCCTTGGCCGTC	63°C
S7	S7RPEX2R**	[20]	AACTCGTCTGGCTTTTCGCC	63°C
RPL3	RPL35F*	[21]	AAGAAGTCYCACCTCATGGAGAT	57.5°C
RPL3	RPL36R**	[21]	TTRCGKGGCAGTTTCTTTGTGTGCCA	57.5°C
GH5	GH5F*	[22]	AGGCCAATCAGGACGGAGC	58.5°C
GH5	GH6R**	[22]	TGCCACTGTCAGATAAGTCTCC	58.5°C
Myo	Mio1F*	[23]	ATGAGCATGCCATCACAGAG	64°C
Myo	Mio1R**	[23]	ATGCGATTGGCTTGAAACTT	64°C
PrI	PrI1F*	[24]	GACAARCTKCACTCBCTCAGCCA	63°C
PrI	PrI1R**	[24]	TGNAGDGAGGABGTGTGRCAC	63°C
ANT	ANTF1*	[25]	TGCTTCGTNTACCCVCTKGACTTTGC	57°C
ANT	ANTR1**	[25]	CCGACTGTCATCATKCGRCGDC	57°C
IGF	FcmugilF*	[26]	GTTACAGCGCCACACAGAC	66°C
IGF	FcmugilR**	[26]	CTTGAAGGATGAATGACTATGTCCA	66°C
Delt8	Delt6F8*	[23]	TTACTACCTTCGCTACCTGTGCT	64°C
Delt8	Delt6R8**	[23]	AGTACCCACACAAACCAGTKAC	64°C
La1	La1F*	[27]	GCTAGCTTTGCATGTTCCC	56°C
La1	La1R**	[27]	AAGGCCTCGCAGATCAATCG	56°C

Control Region (CR), Cytochrome B (Cyt B), Nad dehydrogenase subunit 4 (ND4), Ribosomal Protein S7-intron 1 (S7), Ribosomal Protein L3- intron 5 (RPL3), Growth Hormone-Intron 5 (GH5), Myostatin-intron 1 (Myo), Prolactin-intron-1 (PrI), ANT1-intron 1 (ANT), Insulin-like Growth Factor (IGF), Delta 6 desaturase-intron 8 (Delta8).

doi:10.1371/journal.pone.0161617.t001

In addition, we used some sequences of Gomes et al. [7] and da Silva et al. [23] (GenBank accession codes: KC123167, KC122929, KC122962- KC122964, KC122981-KC122982, KC122989-KC122990, KC123050-KC123057, KC123065-KC123068, KC123071-KC123072, KC123074, KC123076, KC123078, KC123091, KC123094, KC123095, KC123097-KC123166 and KT869380-KT869392, KT869423-KT869425, KT869476-KT869485).

### Databases

After sequencing the genomic regions, the chromatograms were analyzed visually using the program BioEdit v. 7.2.5 [29], in which the sequences were automatically aligned using the application CLUSTAL W [30]. For the nuclear markers, insertion or deletion heterozygosity events were resolved using the Mixed Sequences Reader (available at: <http://MSR.cs.nthu.edu.tw/>) [31].

In nuDNA, the gametic phase of the individuals was determined using the Phase v.2.1 algorithm [32]. We conducted five runs using different random seeds for check consistency of results in each run, each chain consisted of 1000 iterations, a thinning interval of 1 and a burn-in of 1000. For subsequent analyses, only haplotypes with probabilities greater than 0.6 were accepted. The input and output files of Phase, were generated using SeqPhase (available at: <http://www.mnhn.fr/jfflot/seqphase>) [33]. The intragenic recombination was estimated using the PhiW test [34], which is available in Splits Tree v. 4.6 [35].

## Population genetic diversity and structure

The frequency of haplotypes (or alleles from nuDNA) in the population, the number of polymorphic sites, and the nucleotide ( $\pi$ ) and haplotypic diversity ( $h$ ) [36] indices were estimated in Arlequin v. 3.5.1.2 [37].

Population structure was first estimated by pairwise  $F_{ST}$  [38] and Analysis of Molecular Variance (AMOVA) [39] using Arlequin v.3.5.1.2 [37] with 10,000 permutations. For pairwise analyses, the  $\alpha$  value was set at the 0.05 critical level via the false discovery rate correction, as proposed by Benjamini & Yekutieli [40].

To visualize the spatial and genealogical relationships between haplotypes (or alleles for nuDNA) were constructed networks using the program Haploviewer [41], based on topologies estimated by Maximum Likelihood, calculated in PhyML v. 3.0 [42] using the evolutionary model estimated in PAUP\* v. 4.0 [43].

A Bayesian analysis of clustering was conducted in Structure v. 2.3.4 [44] to estimate the ideal number of existing populations. Only the nuclear data were used in this approach. Values of  $K$  between 1 and 6 were tested, and for each value of  $K$ , 10 chains were processed. Each chain had  $10^6$  major steps, with 10% discarded as burn-in. The  $K$  number was inferred by comparing the mean probability values for the data and the variance for each  $K$ . These indices were obtained using Structure Harvester (available at: <http://taylor0.biology.ucla.edu/structureHarvester>) [45].

Bayesian clustering analysis was also conducted in Structurama v. 2.0 [46], and both the mitochondrial and nuclear data were clustered. The runs consisted of  $2 \times 10^6$  steps and 10% of burn-in; the search for the  $K$ -value was performed using the following distribution:  $K = \expk(2)$ .

## Neutrality and demographic history

The fit of the data to the neutral model was tested using the  $F_s$  [47] and  $D$  statistics [48]. These tests were developed to detect deviations caused by selective pressures. However, these statistics are affected by historical demographic fluctuation events and are also widely used to detect these processes, especially the values of  $F_s$  [47,49]. The  $p$ -value for each of these indices was estimated using 10,000 permutations in Arlequin v. 3.5.1.2 [37].

The dynamics of the effective population size over time was estimated using a non-parametric method—Bayesian Skygrid analysis [50]—available in BEAST v. 1.8.0 [51]. A strict clock with a rate of 0.05 sites/million years/within lineages for the control region was used, as in Zhang et al. [52]. The evolutionary model was chosen based on the model proposed by PAUP\* [43] using the Bayesian information criterion (BIC) [53]. The Bayesian Skygrid estimates accommodate multiple loci; therefore, the analysis was conducted for all the sequenced regions, except for ANT1 and La1 because of the low polymorphism rate and the evolutionary model deviating from the infinite sites model, respectively.

For Bayesian Skygrid analysis, were performed two runs with different random seeds. Each chain consisted of  $2.5 \times 10^8$  generations of MCMC, with 10% of this value discarded as burn-in. These runs were conducted on the CIPRES Science Gateway XSEDE server (available at: [http://www.phylo.org/sub\\_sections/portal/](http://www.phylo.org/sub_sections/portal/)) [54]. Mixing and convergence between runs was detected using Tracer v. 1.6 (available at: <http://beast.bio.ed.ac.uk/tracer>) by Effective Sample Size (ESS) values. All the ESS values were greater than 200. The Bayesian Skygrid graphical representation was produced using scripts of Heled [55].

“Bayesian skyline” analyses frequently produce trajectories with increasing or decreasing effective sizes that are not always the most likely scenarios compared to models with constant population size (e.g., [56]). Therefore, the Bayesian Skygrid was compared to a stable

population scenario produced by Beast (using a tree prior of constant population size, and the same parameters listed above). Comparisons between the two scenarios were performed using the Bayes Factor (BF), with the marginal probabilities generated by Path Sampling (PS) and Stepping-Stone (SS) Sampling [57] with  $6 \times 10^6$  generations, 100 paths, and sampling at each 1000<sup>th</sup> generation.

## Results

### Characterization of databases and genetic diversity

In this study, 12 fragments (three mitochondrial and nine nuclear) were sequenced, for a total of 4,224 basepairs (bp), with 2,526 bp from the nuclear regions and 1,698 bp from the mitochondrial regions (S1 Table). The number of individuals sequenced (N), the size of the fragments obtained (bp), the number of haplotypes (Nh) and the number of polymorphic sites (S) are listed in S1 Table.

For the mitochondrial database, high levels of genetic diversity were found, with values between  $0.787 \pm 0.033$  (ND4) and  $0.997 \pm 0.001$  (Control Region) for haplotypic diversity and between  $0.003 \pm 0.002$  (ND4) and  $0.029 \pm 0.014$  (Control Region) for nucleotide diversity (S1 Table). Similarly, high levels of genetic variation were also observed for the majority of the nuclear regions, as the indices for haplotype and nucleotide diversity ranged from  $0.099 \pm 0.030$  (ANT1)–  $0.983 \pm 0.002$  (S7) and  $0.0003 \pm 0.0006$  (ANT1)–  $0.019 \pm 0.011$  (RPL3), respectively (S1 Table). Evidence of intragenic recombination was not found.

### Population genetic structure

The genealogical relationships between haplotypes show a diffuse pattern and are distributed randomly along the studied area (Fig 2), thus indicating possible genetic homogeneity for the area included in this study. In addition, the classic connectivity estimators between populations are congruent to demonstrate a high degree of horizontal genetic connectivity across the entire region studied. For example, for almost all the pairwise  $F_{ST}$  comparisons performed, low and non-significant values were obtained (except for the comparison between CNB1 and Ceará, where  $G_{H5}-F_{ST} = 0.067$ ) (Fig 3). Similarly, according to the AMOVA, the majority of the variance in the data is attributed to the component of variation within and not between populations. Except for GH5, all the st global  $\Phi_{st}$  values are low and non-significant (Fig 4).

The scenario of genetic homogeneity across the region studied is also corroborated by Bayesian clustering analysis of individuals, the scenario with a single large group is supported (Structurama  $K1 = 0.94$ ; S2 Table). Therefore, the existence of high levels of genetic homogeneity for *L. purpureus* along the Brazilian coast is supported in accordance with previous studies using mtDNA [6,7].

### Neutrality and demographic history

The neutrality estimators were negative and significant for Tajima's  $D$  and Fu's  $F_s$  for all the mitochondrial markers. For the nuclear regions, the majority of the segments analyzed had negative and significant  $F_s$  values (S1 Table). However, for  $D$ , significant deviations from the neutral model were found only for ANT1 ( $-1.321$ ;  $p < 0.05$ ) and La1 ( $-2.147$ ;  $p < 0.05$ ). Despite this, a population expansion event cannot be ruled out, because autosomal markers are generally less sensitive for detecting demographic fluctuation events due to their larger effective sizes compared to mitochondrial DNA. Additionally,  $F_s$  has a greater statistical power for detecting deviations from neutrality caused by demographic changes [45].

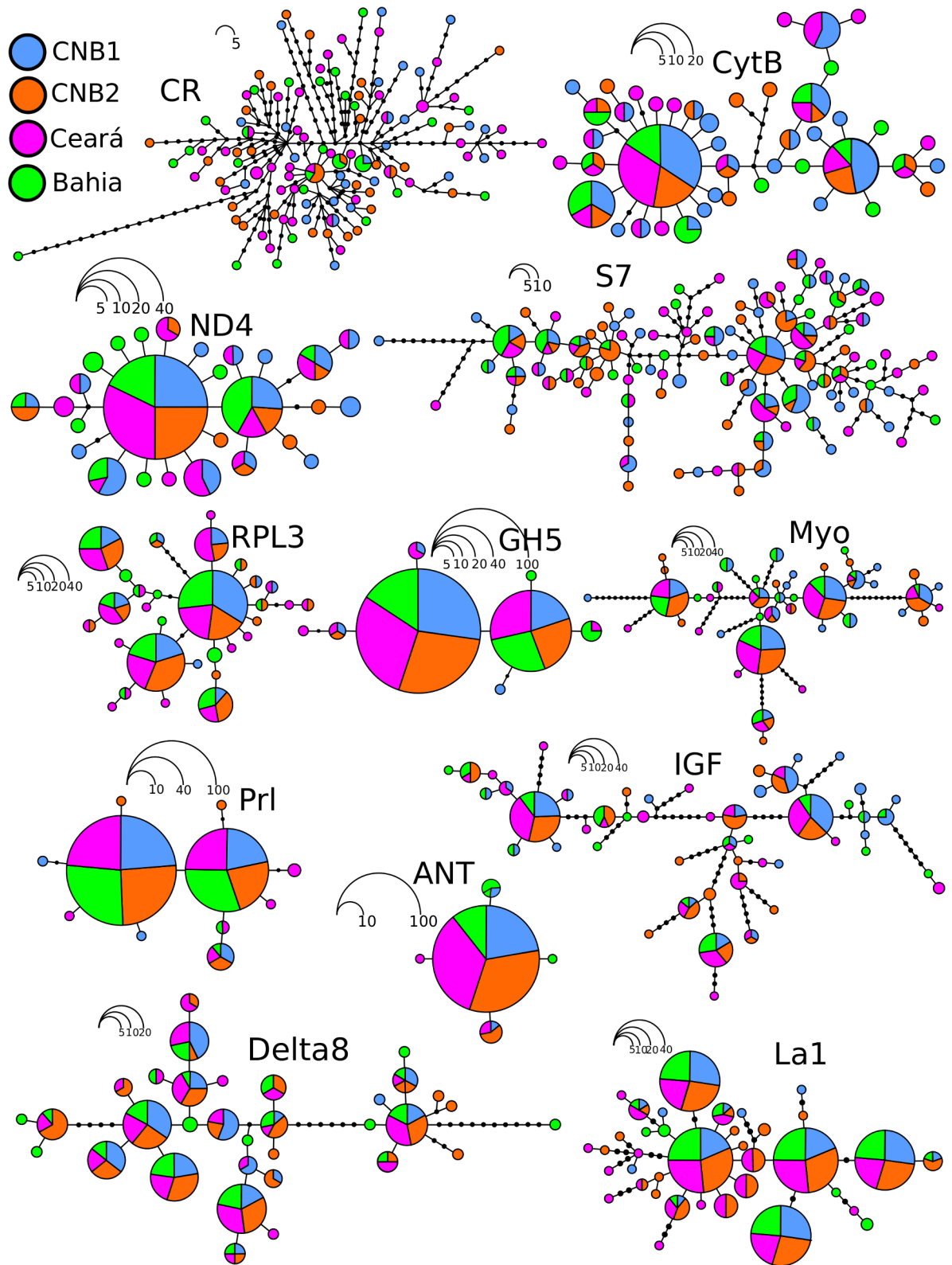


**Fig 2. Genealogical relationships between haplotypes of the loci used in this study.** Each circle represents a haplotype, and the area is proportional to the frequency of the haplotype. Colors refer to the collection location.

doi:10.1371/journal.pone.0161617.g002

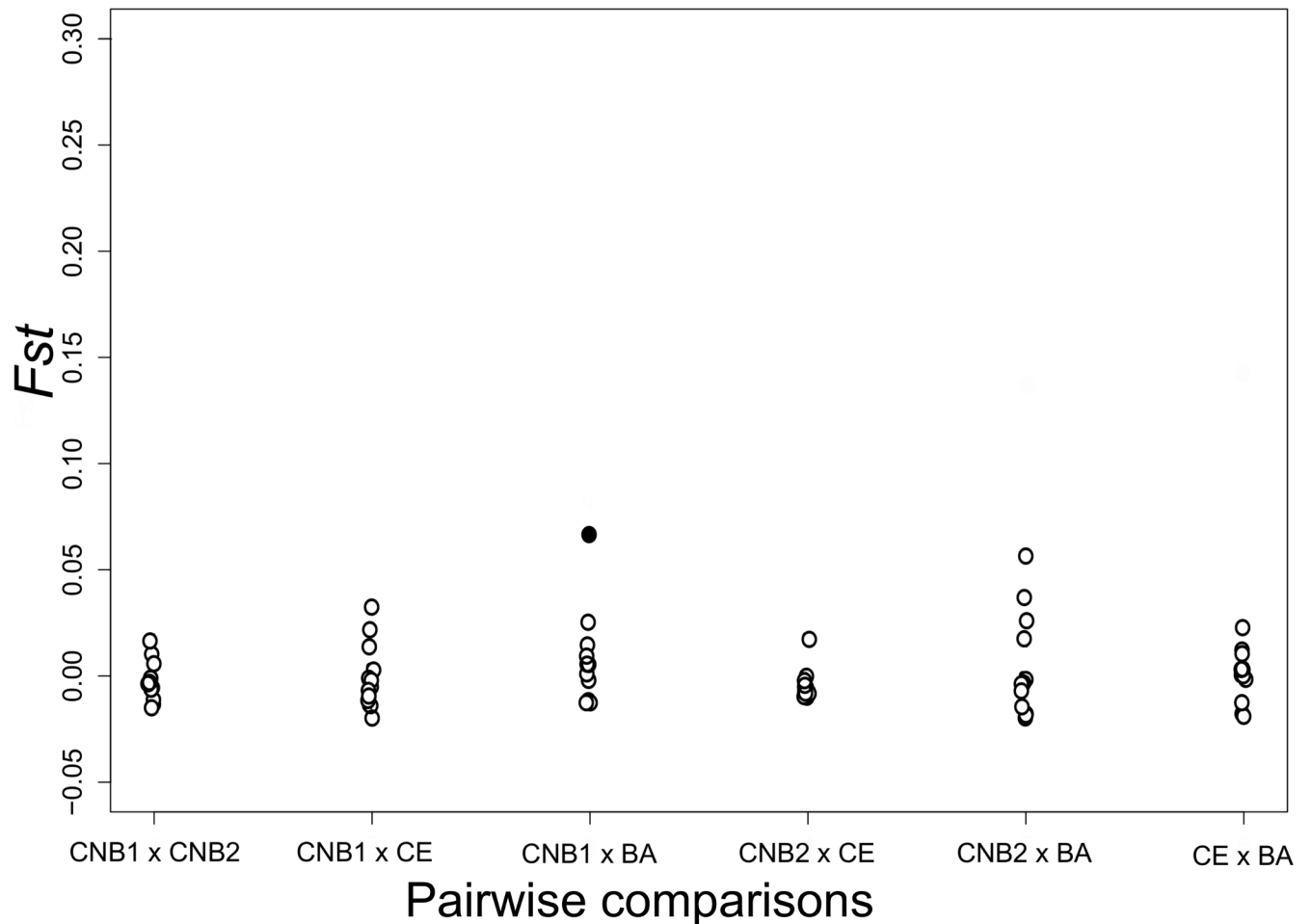


**Fig 3. Comparisons of pairwise  $F_{ST}$  between sampling locations and the loci used in this study.** Open circles represent non-significant  $F_{ST}$  after FDR correction (i.e.,  $p > 0.02$ ). Filled circles represent  $p < 0.02$  (GH5).

doi:10.1371/journal.pone.0161617.g003

Also in relation to the demography scenario, the comparison of the marginal probabilities between the Bayesian Skygrid and a constant population provided very strong evidence for the Skygrid model (Skygrid Bayes Factor  $\geq 30$ ; Fig 5) [58]. Bayesian Skygrid analysis revealed an approximately ten-fold increase in the effective *L. purpureus* population size, which began approximately 150 thousand years ago (Fig 6). This demographic expansion event may be related to increases and decreases in sea level during the Pleistocene, as this dating coincides with a period of glacial maximum in the Tropical Atlantic [59].

## Discussion

### Genetic diversity

Historically, genetic diversity estimators have been widely cited as indicators of adaptability and persistence for natural populations [60]. There are many examples of direct relationship between genetic diversity and effective population size; commonly large populations exhibit high levels of genetic diversity (reviewed in [61]).

This study found high levels of genetic diversity in a large portion of the genomic regions analyzed. This pattern is very similar to what has been observed in other marine organisms



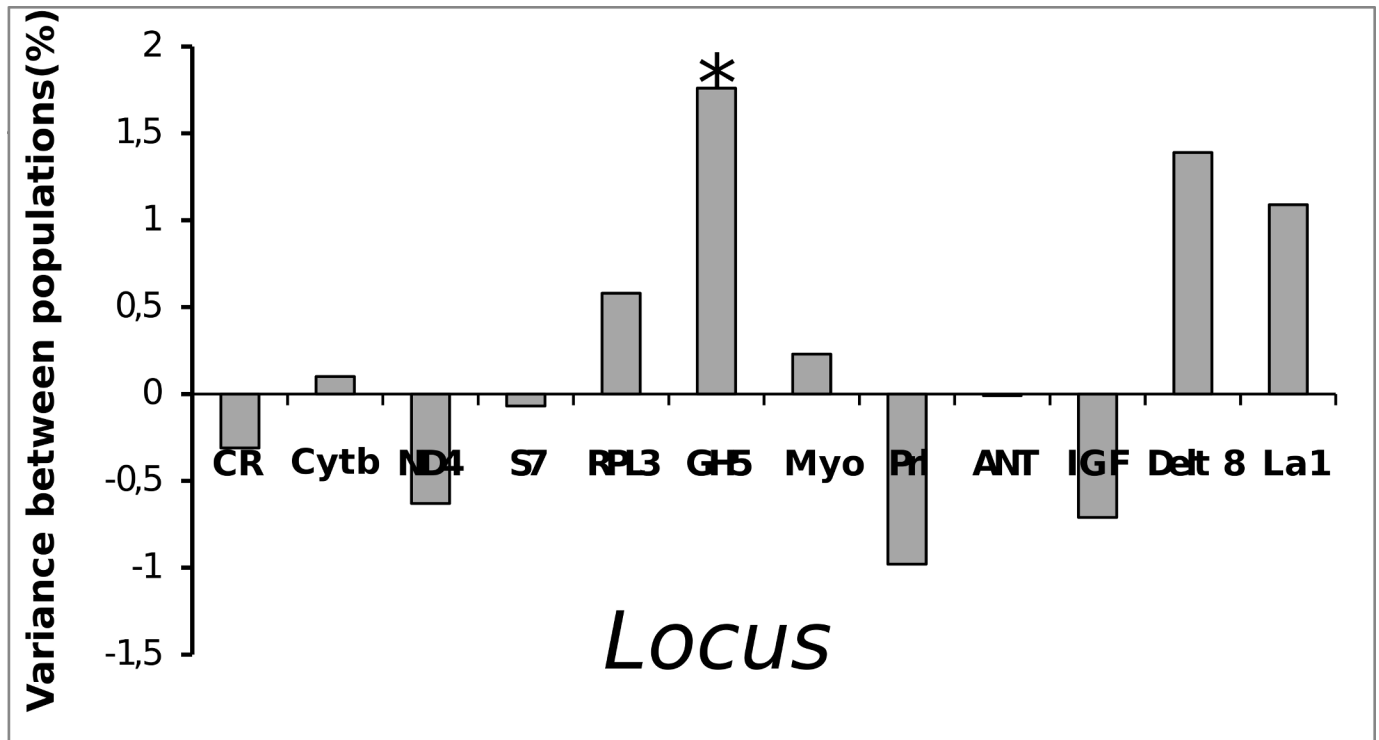


**Fig 4. Proportion of the variance (in percentage) between populations when all the sampled locations are grouped into a single cluster. \***-  $\Phi_{st}$  value is significant ( $p < 0.05$ ).

doi:10.1371/journal.pone.0161617.g004

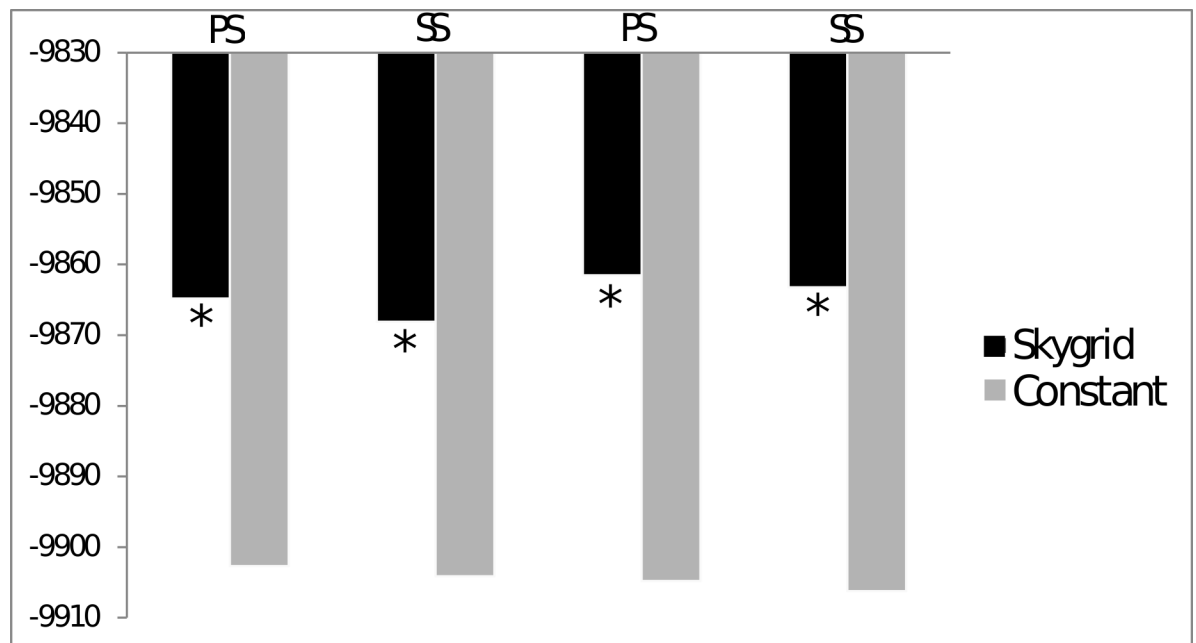


**Fig 5. Estimates of the marginal probability values inferred by Path Sampling (PS) and Stepping-Stone (SS) Sampling.** Values on the y-axis represent the marginal probability (in ln). Asterisks indicate strong evidence (i.e., Bayes Factor > 10) favoring one of the scenarios: Skygrid or stable population.

doi:10.1371/journal.pone.0161617.g005

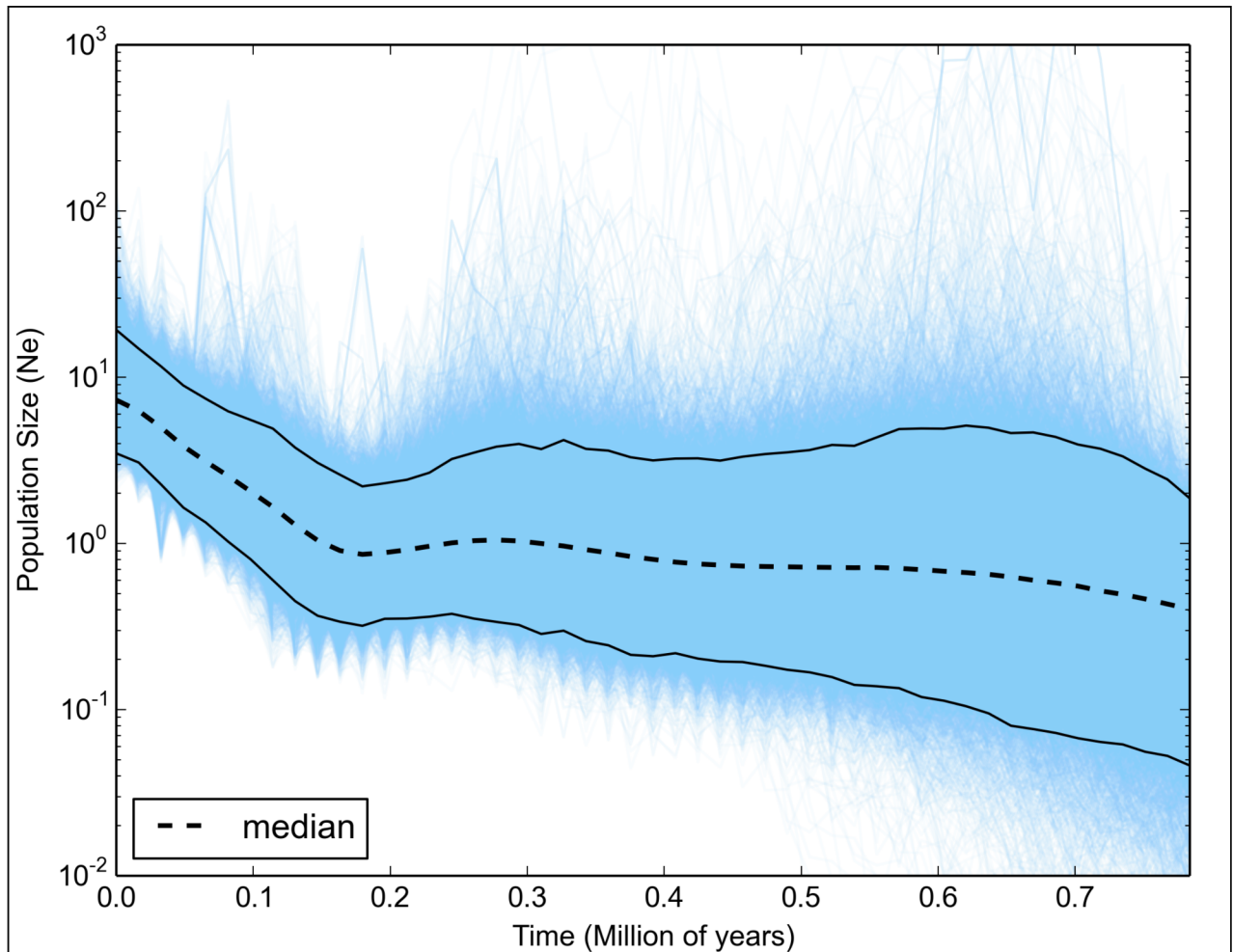


**Fig 6. Population dynamics for *L. purpureus* taken from the Brazilian coast estimated by Bayesian Skygrid analysis.** The x-axis shows time (in million years). The y-axis shows the product of the effective population size and generation time.

doi:10.1371/journal.pone.0161617.g006

(see [62]), including members of the Lutjanidae family, such as *Lutjanus campechanus* (Poey 1860) [63] and *Ocyurus chrysurus* (Bloch 1790) [64], as well as reported by Gomes et al. [7] for *L. purpureus*.

The Caribbean snapper *L. purpureus* has experienced fishing pressure for more than half a century [65], and there are several examples of species with decreased genetic diversity due to overfishing (see [66]). However this tendency appears to be more evident in species with small  $N_e$ , (e.g., several hundred) and that have some type of population subdivision [66]. This trend clearly is not the case with *L. purpureus* along the Brazilian coast, as it has high genetic diversity and therefore likely to have a high  $N_e$ ; however, large population sizes do not mean that fishing is not affecting the populations. Several methods to estimate the effective population size appear to not reflect the current population size for species that are excessively fished, but still reflect the population dynamics prior to fishing (e.g., [67]). In addition, even if these populations currently have large  $N_e$  values, they are more susceptible to the loss of alleles if individuals are removed excessively compared to populations with smaller  $N_e$  values [68]. Therefore, it would not be appropriate to dismiss the effects that overfishing can have on *L. purpureus* stocks, despite the high levels of genetic diversity observed.

## Population structure and genetic connectivity

In this study, both the  $F$ -statistics, the Bayesian clustering and coalescent estimates of effective migration strongly support a scenario of genetic homogeneity for *L. purpureus* in the South-west Atlantic.

For many marine species, the scenario of high genetic connectivity is mainly attributed to the apparent lack of dispersal barriers [1]. Additionally, the life history of the species also has a direct influence on maintaining genetic connectivity among populations. For example, the pelagic larval duration (PLD) and egg type (pelagic), two characteristics of snapper reproductive biology/ life history, have been both cited as promoters of genetic connectivity in the marine environment [69–71]. Additionally, species with deeper vertical distributions apparently have higher levels of genetic connectivity than pelagic species [2].

*L. purpureus* individuals are generally found on the continental slope [72] usually associated with substrate at depths of up to 160 meters [4,13]. Spawning occurs over oceanic banks, and the eggs are pelagic [4]. There are no data available on the duration of the initial pelagic larval stage, but it is most likely approximately 30 days long, which is very common for lutjanids in the tropical Atlantic [5]. Thus, the larvae remain passive to ocean currents for a long period of time [5]. These characteristics are consistent with the high levels of genetic connectivity observed and are consistent with previous reports on the species [6,7].

In addition, ocean currents appear to play an essential role in genetic connectivity in the Tropical Atlantic (e.g., [73–75]). In this region, the dynamics of ocean circulation are mainly influenced by the bifurcation of the South Equatorial Current, which creates the Brazilian and North Brazilian currents [76]. However, for several groups, this branching does not appear to affect genetic flow [77–79].

These two oceanic currents change slightly across seasons (see [http://www.aoml.noaa.gov/phod/graphics/dacdata/seasonal\\_brazil.gif](http://www.aoml.noaa.gov/phod/graphics/dacdata/seasonal_brazil.gif)), which may facilitate connectivity in the region studied. Additionally, data collected for drifters show that floating objects can cross the study region in a little more than a month (see [S1 File](#)) thus, it would be possible to maintain genetic connectivity over the region by larval dispersion mediated by currents. Thus, all the data support the scenario of high genetic homogeneity shown here.

Hauser and Carvalho, Carvalho and Hauser [80,81] have cited the sampling in the areas of spawning as one of the main factor for accurate determining of population structure in marine fishes. Here, we used samples collected between 2003–2010 in areas of non-spawning. However, tests of bayesian clustering (which only use genetic information for clustering) did not detect any evidence of genetic subdivision. Hence, our scheme of sampling does not seem to have had a great impact on the apparent lack of spatial subdivision in *L. purpureus* observed here.

Marine fish generally have high effective population sizes [61,62,82], thus, even in populations that have some sort of restricted genetic flow, molecular markers of “neutral” evolution may fail to reveal genetic differentiation [82], as there is an inverse relationship between lineage sorting and effective population size for neutral markers. Therefore, for a scenario of genetic homogeneity, as detected in this study, it is difficult to distinguish between populations with recent histories and/or with subtle genetic breaks and those with continuous panmixia.

## Demographic history

Studies on the demographic histories of several marine organisms have shown situations where historical climatic events have lead to contraction and/or expansion of populations. Several of these types of events have been reported for lutjanids, such as *Lutjanus erythropterus* (Bloch 1790) [52], *L. campechanus* [83], *O. chrysurus* [84] and *L. purpureus* [6,7]. The present study

found several pieces of evidence supporting a historical expansion of the effective population size of *L. purpureus*. Significant negative values for the tests of neutrality were measured for a large portion of the loci used here, which may be due to deviations from neutrality caused by population expansion (e.g. [85]). It is known, however, that demographic fluctuations and selection have similar signatures within a given genealogy [86], but the effects of selection are restricted to specific regions in the genome. In contrast, demographic fluctuations affect the genome more uniformly [86]; thus, analyzing multiple loci allows for distinguishing between stochastic demographic processes and selection [87].

Not all the tests and/or genomic regions revealed deviations from the neutral evolution model. Thus, one possible explanation is that the significant negative values for  $F_s$  and  $D$  presented here result from selection and not fluctuations in effective population size. However, because the  $N_e$  was four times larger compared to mitochondrial DNA, the autosomal loci reflect ancestral evolutionary histories; therefore, autosomal regions often fail to show deviations from neutrality caused by fluctuations in effective population size [87,88]. Thus, the scenario involving demographic expansion and deviation in some of the neutrality estimators (i.e., only the mitochondrial markers) is very common in many vertebrate groups [87].

The Bayesian Skygrid analysis clearly showed a growth curve with the effective population size increasing ten-fold (as this scenario is highly supported by comparison of marginal probabilities) beginning approximately 150 thousand years ago, congruent with a glacial maximum period [59]. Similarly, it has been reported that various other teleosts in the Atlantic, including lutjanids, appear to have undergone demographic expansion due to sea level oscillations in the Pleistocene. This seems true for *Cynoscion guatucupa* (Cuvier 1830) [89], *O. chrysurus* [84] and *Lutjanus synagris* (Linnaeus 1758) (G. Gomes, pers. obser.).

However, we used a phylogenetically derived mutation rate, which can sometimes result in erroneous inferences of demographic events, hence the age estimate of the population expansion event should be interpreted with caution, because of time-dependence of molecular clock (Grant [90] and the references therein).

Due to decreasing sea levels, large portions of the continental shelf became exposed, reducing the amount of available habitat and resources for coastal species [91]. Species whose population dynamics were strongly affected by glaciation events typically have reduced genetic diversity values and shallow star-shaped genealogies [91], which is much different than what was found for *L. purpureus*, which has high levels of genetic diversity for most of the loci sampled. However, exemplars of *L. purpureus* are frequently found on the continental slope, at depths of up to 130 meters [72]. Therefore, a decrease in sea level would have a reduced effect on resource availability for this species, lessening the effects of glacial maximum events on genetic variability and historical population dynamics compared to species with more coastal distributions.

## Final considerations

Molecular markers have provided extensive information on the historical population dynamics of various groups of organisms (e.g., [92]). For species widely targeted for commercial fishing, these data are essential to better understand the effects of commercial harvesting on natural stocks [8]. The inclusion of new genomic regions of the present study shows some agreement to previous studies for *L. purpureus*, using single mtDNA region [7]. However the use of the multiple markers seems less biased by gene tree histories. Thereby, further studies involving neutral and non-neutral molecular markers (e. g. SNPs, adaptive loci), should be conducted to better understand the role of natural selection and neutral processes in *L. purpureus*.

The results obtained here, show that *L. purpureus* maintain high levels of genetic diversity, probably a reflex of the large effective population size of the species. However, these findings

should not be understood as evidence of a lack of overfishing effects on the snapper populations, as this activity is recent. Additionally, given the large effective population size of this species, the effects of this activity on genetic diversity may not be detectable.

In addition, *L. purpureus* is genetically homogeneous across the region studied, which may contribute to the high levels of genetic diversity present there [62]. It is also difficult to distinguish between scenarios with continuous panmixia and/or subtle interruptions in genetic flow in species with large effective population sizes (i.e., eurimixia *sensu* Dawson et al. [93]). Nevertheless, similar genetic homogeneity levels are frequently reported for species that, similar to *L. purpureus*, have an initial larval dispersal period and spawn in the open ocean [69,71]. Thus, these factors appear to support the apparent horizontal genetic homogeneity across the region studied.

## Supporting Information

**S1 File. Data about movement of drifters from Brazilian coast (web address).**  
(DOC)

**S1 Table. Characterization of the polymorphism rates and neutrality indices for the genomic regions studied here.**  
(DOCX)

**S2 Table. Distribution of mean probability values for the data (in ln), for each value of K estimated here (1–6). The highest probability values and lower variance when K = 1.**  
(DOCX)

## Author Contributions

**Conceptualization:** RS IS HS GG.

**Formal analysis:** RS.

**Funding acquisition:** IS HS GG.

**Investigation:** RS GG.

**Methodology:** RS GG.

**Project administration:** IS HS GG.

**Resources:** IS HS GG.

**Supervision:** IS HS GG.

**Validation:** RS GG.

**Visualization:** RS IS HS GG.

**Writing – original draft:** RS GG.

**Writing – review & editing:** RS IS HS GG.

## References

1. Palumbi SR. Genetic Divergence, Reproductive Isolation, and Marine Speciation. *Annu Rev Ecol Syst.* 1994; 25: 547–572.
2. Selkoe KA, Gaggiotti OE, TOBOLaboratory, Bowen BW, Toonen R. Emergent patterns of population genetic structure for a coral reef community. *Mol Ecol.* 2014; 23: 3064–3079. doi: [10.1111/mec.12804](https://doi.org/10.1111/mec.12804) PMID: [24866831](https://pubmed.ncbi.nlm.nih.gov/24866831/)

3. Moura RL, Lindeman KC. A new species of snapper (Perciformes: Lutjanidae) from Brazil, with comments on the distribution of *Lutjanus griseus* and *L. apodus*. *Zootaxa*. 2007; 43: 31–43.
4. Fonteles-Filho AA. Síntese sobre a distribuição, Abundância, Potencial Pesqueiro, e Biologia do pargo, *Lutjanus purpureus*, Poey da Zona Econômica Exclusiva do Nordeste do Brasil. Brasília; 2000.
5. Lindeman KC, Lee TN, Wilson WD, Claro R, Ault JS. Transport of Larvae Originating in Southwest Cuba and Dry Tortugas: Evidence for Retention in Grunts and Snappers. *Proc 52nd Gulf Caribb Fish Inst*. 2001;52: 732–747.
6. Gomes G, Schneider H, Vallinoto M, Santos S, Orti G, Sampaio I. Can *Lutjanus purpureus* (South red snapper) be “legally” considered a red snapper (*Lutjanus campechanus*)? *Genet Mol Biol*. 2008; 31: 372–376.
7. Gomes G, Sampaio I, Schneider H. Population structure of *Lutjanus purpureus* (Lutjanidae—Perciformes) on the Brazilian coast: further existence evidence of a single species of red snapper in the western Atlantic. *An Acad Bras Cienc*. 2012; 84: 979–999. PMID: [23207703](#)
8. Ovenden JR, Berry O, Welch DJ, Buckworth RC, Dichmont CM. Ocean’s eleven: a critical evaluation of the role of population, evolutionary and molecular genetics in the management of wild fisheries. *Fish Fish*. 2013; 1–35.
9. Nielsen R, Beaumont MA. Statistical inferences in phylogeography. *Mol Ecol*. 2009; 18: 1034–1047. doi: [10.1111/j.1365-294X.2008.04059.x](#) PMID: [19207258](#)
10. Heled J, Drummond AJ. Bayesian inference of population size history from multiple loci. *BMC Evol Biol*. 2008; 8: doi: [10.1186/1471-2148-8-289](#)
11. Eytan RI, Hellberg ME. Nuclear and mitochondrial sequence data reveal and conceal different demographic histories and population genetic processes in Caribbean reef fishes. *Evolution*. 2010; 64: 3380–3397. doi: [10.1111/j.1558-5646.2010.01071.x](#) PMID: [20584072](#)
12. Pritchard JK, Wen X, Falush D. Documentation for structure software: Version 2.3. 2010.
13. Allen G-R. Snappers of the World. An annotated and illustrated catalogue of Lutjanid species known to date. Vol 6. Rome: FAO. 208 p; 1985.
14. Wessel P, Smith WHF, Scharroo R, Luis J, Wobbe F. Generic Mapping Tools: Improved version released. *EOS Trans AGU*. 2013; 94: 409–410.
15. Sambrook J, Fritsch EF, Maniatis T. Molecular cloning: a laboratory manual. New York: Cold Spring Harbor Laboratory Press; 1989.
16. Lee W-J, Conroy J, Howell WH, Kocher TD. Structure and Evolution of Teleost Mitochondrial Control Regions. *J Mol Evol*. 1995; 41: 54–66. PMID: [7608989](#)
17. Sevilla RG, Diez A, Norén M, Mouchel O, Jérôme M, Verrez-Bagnis V, et al. Primers and polymerase chain reaction conditions for DNA barcoding teleost fish based on the mitochondrial cytochrome b and nuclear rhodopsin genes. *Mol Ecol Notes*. 2007; 7: 730–734.
18. Bielawski JP, Gold JR. Mutation patterns of mitochondrial H- and L-strand DNA in closely related Cyprinid fishes. *Genetics*. 2002; 161: 1589–1597. PMID: [12583346](#)
19. Arevalo E, Davis SK, Sites JW. Mitochondrial DNA Sequence Divergence and Phylogenetic Relationships among Eight Chromosome Races of the *Sceloporus grammicus* Complex (Phrynosomatidae) in Central. *Syst Biol*. 1994; 43: 387–418.
20. Chow S, Hazama K. Universal PCR primers for S7 ribosomal protein gene introns in fish. *Mol Ecol*. 1998; 7: 1247–1263.
21. Pinho C, Rocha S, Carvalho BM, Lopes S, Mourão S, Vallinoto M, et al. New primers for the amplification and sequencing of nuclear loci in a taxonomically wide set of reptiles and amphibians. *Conserv Genet Resour*. 2009; 2: 181–185.
22. Hassan M, Lemaire C, Fauvelot C, Bonhomme F. Seventeen new exon-primed intron-crossing polymerase chain reaction amplifiable introns in fish. *Mol Ecol Notes*. 2002; 2: 334–340.
23. Da Silva R, Silva D, Veneza I, Sampaio I, Schneider H, Gomes G. Development of Intragenic Markers and Their Applicability in Population Analyses of Lutjanidae (Perciformes). *An Acad Bras Cienc*. In press.
24. Blel H, Panfili J, Guinand B, Berrebi P, Said K, Durand J. Selection footprint at the first intron of the Prl gene in natural populations of the flathead mullet (*Mugil cephalus*, L. 1758). *J Exp Mar Bio Ecol*. 2010; 387: 60–67.
25. Jarman SN, Ward RD, Elliott NG. Oligonucleotide primers for PCR amplification of Coelomate introns. *Mar Biotechnol*. 2002; 4: 347–355. PMID: [14961246](#)
26. Rodrigues-Filho LFS. Identificação e Filogeografia de Tainhas do Gênero *Mugil* e avaliação do estado taxonomico das espécies *Mugil liza* Valenciennes, 1836 e *Mugil platanus* Günther, 1880. Universidade Federal do Pará. Ph. D. Thesis, 2011.

27. Zhang J, Cai Z, Huang H. Isolation and characterization of microsatellite loci from mangrove red snapper *Lutjanus argentimaculatus*. *Mol Ecol Notes*. 2006; 6: 408–411.
28. Sanger F, Nicklen S, Coulson AR. DNA sequencing with chain-terminating inhibitors. *Proceedings Natl Acad Sci USA*. 1977; 74: 5463–5467.
29. Hall TA. BioEdit: A user-friendly biological sequence alignment editor and analysis program for Windows 95/98/NT. *Nucleic Acids Symp Ser*. 1999; 41: 95–98.
30. Thompson JD, Gibson TJ, Plewniak F, Jeanmougin F, Higgins DG. The CLUSTAL\_X windows interface: flexible strategies for multiple sequence alignment aided by quality analysis tools. *Nucleic Acids Res*. 1997; 25: 4876–4882. PMID: [9396791](#)
31. Chang C-T, Tsai C-N, Tang CY, Chen C-H, Lian J-H, Hu C-Y, et al. Mixed sequence reader: a program for analyzing DNA sequences with heterozygous base calling. *Sci World J*. 2012; 2012: 365104.
32. Stephens M, Donnelly P. A comparison of bayesian methods for haplotype reconstruction from population genotype data. *Am J Hum Genet*. 2003; 73: 1162–1169. PMID: [14574645](#)
33. Flot J-F. Seqphase: a Web Tool for Interconverting Phase Input/Output Files and Fasta Sequence Alignments. *Mol Ecol Resour*. 2010; 10: 162–166. doi: [10.1111/j.1755-0998.2009.02732.x](#) PMID: [21565002](#)
34. Bruen TC, Philippe H, Bryant D. A simple and robust statistical test for detecting the presence of recombination. *Genetics*. 2006; 172: 2665–2681. PMID: [16489234](#)
35. Huson DH, Bryant D. Application of phylogenetic networks in evolutionary studies. *Mol Biol Evol*. 2006; 23: 254–267. PMID: [16221896](#)
36. Nei M. *Molecular Evolutionary Genetics*. New York: Columbia Univ. Press. 512 p; 1987.
37. Excoffier L, Lischer HEL. Arlequin suite ver 3.5: a new series of programs to perform population genetics analyses under Linux and Windows. *Mol Ecol Resour*. 2010; 10: 564–567. doi: [10.1111/j.1755-0998.2010.02847.x](#) PMID: [21565059](#)
38. Weir BS, Cockerham CC. Estimating F-statistics For Population Structure. *Evolution*. 1984; 38: 1358–1370.
39. Excoffier L, Smouse PE, Quattro JM. Analysis of Molecular Variance Inferred from Metric Distances among DNA Haplotypes: Application to Human Mitochondrial DNA Restriction Data. *Genetics Soc America*; 1992; 131: 479–491.
40. Benjamini Y, Yekutieli D. The control of the false discovery rate in multiple testing under dependency. *Ann Stat*. 2001; 29: 1165–1188.
41. Salzburger W, Ewing GB, von Haeseler A. The performance of phylogenetic algorithms in estimating haplotype genealogies with migration. *Mol Ecol*. 2011; 20: 1952–1963. doi: [10.1111/j.1365-294X.2011.05066.x](#) PMID: [21457168](#)
42. Guindon S, Dufayard J-F, Lefort V, Anisimova M, Hordijk W, Gascuel O. New algorithms and methods to estimate maximum-likelihood phylogenies: assessing the performance of PhyML 3.0. *Syst Biol*. 2010; 59: 307–321. doi: [10.1093/sysbio/syq010](#) PMID: [20525638](#)
43. Swofford DL. PAUP, Phylogenetic Analysis Using Parsimony and other Methods. Beta Version V 4.10b. Sunderland, Massachusetts: Sinauer Associates; 2002.
44. Pritchard JK, Stephens M, Donnelly P. Inference of population structure using multilocus genotype data. *Genetics*. 2000; 155: 945–959. PMID: [10835412](#)
45. Earl DA, VonHoldt BM. STRUCTURE HARVESTER: a website and program for visualizing STRUCTURE output and implementing the Evanno method. *Conserv Genet Resour*. 2011; 4: 359–361.
46. Huelsenbeck JP, Andolfatto P, Huelsenbeck ET. Structurama: bayesian inference of population structure. *Evol Bioinforma*. 2011; 7: 55–59.
47. Fu Y-X. Statistical Tests of Neutrality of Mutations Against Population Growth, Hitchhiking and Background Selection. *Genetics*. 1997; 147: 915–925. PMID: [9335623](#)
48. Tajima F. Statistical method for testing the neutral mutation hypothesis by DNA polymorphism. *Genetics*. 1989; 123: 585–595. PMID: [2513255](#)
49. Ramírez-Soriano A, Ramos-Onsins SE, Rozas J, Calafell F, Navarro A. Statistical power analysis of neutrality tests under demographic expansions, contractions and bottlenecks with recombination. *Genetics*. 2008; 179: 555–567. doi: [10.1534/genetics.107.083006](#) PMID: [18493071](#)
50. Gill MS, Lemey P, Faria NR, Rambaut A, Shapiro B, Suchard MA. Improving Bayesian Population Dynamics Inference: A Coalescent-Based Model for Multiple Loci. *Mol Biol Evol*. 2013; 30: 713–724. doi: [10.1093/molbev/mss265](#) PMID: [23180580](#)
51. Drummond AJ, Suchard MA, Xie D, Rambaut A. Bayesian phylogenetics with BEAUti and the BEAST 1.7. *Mol Biol Evol*. 2012; 29: 1969–1973. doi: [10.1093/molbev/mss075](#) PMID: [22367748](#)

52. Zhang J, Cai Z, Huang L. Population genetic structure of crimson snapper *Lutjanus erythropterus* in East Asia, revealed by analysis of the mitochondrial control region. *ICES J Mar Sci.* 2006; 63: 693–704.
53. Schwarz G. Estimating the Dimension of a Model. *Ann Stat.* 1978; 6: 461–464.
54. Miller MA, Pfeiffer W, Schwartz T. Creating the CIPRES Science Gateway for inference of large phylogenetic trees. 2010 Gatew Comput Environ Work. *IEEE*; 2010; 1–8. doi: [10.1109/GCE.2010.5676129](https://doi.org/10.1109/GCE.2010.5676129)
55. Heled J. Extended Bayesian Skyline Plot tutorial [Internet]. 2010. Available: <http://beast.bio.ed.ac.uk/tutorials>
56. O'Brien SM, Gallucci VF, Hauser L. Effects of species biology on the historical demography of sharks and their implications for likely consequences of contemporary climate change. *Conserv Genet.* 2013; 14: 125–144.
57. Baele G, Lemey P, Bedford T, Rambaut A, Suchard MA, Alekseyenko A V. Improving the accuracy of demographic and molecular clock model comparison while accommodating phylogenetic uncertainty. *Mol Biol Evol.* 2012; 29: 2157–2167. doi: [10.1093/molbev/mss084](https://doi.org/10.1093/molbev/mss084) PMID: [22403239](https://pubmed.ncbi.nlm.nih.gov/22403239/)
58. Kass RE, Raftery AE. Bayes Factors. *J Am Stat Assoc.* 1995; 90: 773–795.
59. Barreto AMF, Bezerra FHR, Suguio K, Tatum SH, Yee M, Paiva RP, et al. Late Pleistocene marine terrace deposits in northeastern Brazil: sea-level change and tectonic implications. *Palaeogeogr Palaeoclimatol Palaeoecol.* 2002; 179: 57–69.
60. Hare MP, Nunney L, Schwartz MK, Ruzzante DE, Burford M, Waples RS, et al. Understanding and estimating effective population size for practical application in marine species management. *Conserv Biol.* 2011; 25: 438–449. doi: [10.1111/j.1523-1739.2010.01637.x](https://doi.org/10.1111/j.1523-1739.2010.01637.x) PMID: [21284731](https://pubmed.ncbi.nlm.nih.gov/21284731/)
61. McCusker MR, Bentzen P. Positive relationships between genetic diversity and abundance in fishes. *Mol Ecol.* 2010; 19: 4852–4862. doi: [10.1111/j.1365-294X.2010.04822.x](https://doi.org/10.1111/j.1365-294X.2010.04822.x) PMID: [20849560](https://pubmed.ncbi.nlm.nih.gov/20849560/)
62. DeWoody JA, Avise JC. Microsatellite variation in marine, freshwater and anadromous fishes compared with other animals. *J Fish Biol.* 2000; 56: 461–473.
63. Garber AF, Tringali MD, Stuck KC. Population structure and variation in red snapper (*Lutjanus campechanus*) from the Gulf of Mexico and Atlantic coast of Florida as determined from mitochondrial DNA control region sequence. *Mar Biotechnol.* 2004; 6: 175–185. PMID: [14586768](https://pubmed.ncbi.nlm.nih.gov/14586768/)
64. Vasconcellos AV, Vianna P, Paiva PC, Schama R, Solé-Cava A. Genetic and morphometric differences between yellowtail snapper (*Ocyurus chrysurus*, Lutjanidae) populations of the tropical West Atlantic. *Genet Mol Biol.* 2008; 31: 308–316.
65. Resende SM, Ferreira BP, Fredou T. A pesca de Lutjanídeos no Nordeste do Brasil: Histórico das Pescarias, Características das Espécies e Relevância para o Manejo. *Bol Técnico Científico da CEPENE.* 2003; 11: 257–270.
66. Pinsky ML, Palumbi SR. Meta-analysis reveals lower genetic diversity in overfished populations. *Mol Ecol.* 2014; 23: 29–39. doi: [10.1111/mec.12509](https://doi.org/10.1111/mec.12509) PMID: [24372754](https://pubmed.ncbi.nlm.nih.gov/24372754/)
67. Alter SE, Rynes E, Palumbi SR. DNA evidence for historic population size and past ecosystem impacts of gray whales. *Proc Natl Acad Sci U S A.* 2007; 104: 15162–15167. PMID: [17848511](https://pubmed.ncbi.nlm.nih.gov/17848511/)
68. Allendorf FW, Berry O, Ryman N. So long to genetic diversity, and thanks for all the fish. *Mol Ecol.* 2014; 23: 23–25. doi: [10.1111/mec.12574](https://doi.org/10.1111/mec.12574) PMID: [24372752](https://pubmed.ncbi.nlm.nih.gov/24372752/)
69. Shulman MJ., Bermingham E. Early Life Histories, Ocean Currents, and the Population Genetics of Caribbean Reef Fishes. *Evolution.* 1995; 49: 897–910.
70. Planes S. Biogeography and Larval Dispersal Inferred from Population Genetic Analysis. In: Sale P., editor. *Coral reef fishes: dynamics and diversity in a complex ecosystem.* New York, USA: Academic Press; 2002. pp. 201–220.
71. Dawson MN. Natural experiments and meta-analyses in comparative phylogeography. Phillimore A, editor. *J Biogeogr.* 2014; 41: 52–65.
72. Furtado-Júnior I, Brito CSF. Biologia e pesca do pargo *Lutjanus purpureus*, Poey, 1875 (Pisces: Lutjanidae), na região Norte do Brasil. *Bol Téc Cient Cepnor.* 2002; 2: 173–190.
73. Santos S, Hrbek T, Farias IP, Schneider H, Sampaio I. Population genetic structuring of the king weakfish, *Macrodon ancylodon* (Sciaenidae), in Atlantic coastal waters of South America: deep genetic divergence without morphological change. *Mol Ecol.* 2006; 15: 4361–4373. PMID: [17107470](https://pubmed.ncbi.nlm.nih.gov/17107470/)
74. Santos S, Schneider H, Sampaio I. Genetic differentiation of *Macrodon ancylodon* (Sciaenidae, Perciformes) populations in Atlantic coastal waters of South America as revealed by mtDNA analysis. *Genet Mol Biol.* 2003; 161: 151–161.
75. Benevides EA, Vallinoto MNS, Fetter Filho AFH, de Souza JRB, Silva-Oliveira G, Freitas MO, et al. When physical oceanography meets population genetics: The case study of the genetic/evolutionary discontinuity in the endangered goliath grouper (*Epinephelus itajara*; Perciformes: Epinephelidae) with comments on the conservation of the species. *Biochem Syst Ecol.* 2014; 56: 255–266.



76. Peterson RG, Stramma L. Upper-level circulation in the South Atlantic Ocean. *Prog Ocean*. 1991; 26: 1–73.
77. Wieman AC, Berendzen PB, Hampton KR, Jang J, Hopkins MJ, Jurgenson J, et al. A panmictic fiddler crab from the coast of Brazil? Impact of divergent ocean currents and larval dispersal potential on genetic and morphological variation in *Uca maracoani*. *Mar Biol*. 2013; 161: 173–185.
78. Rodríguez-Rey GT, Solé-Cava AM, Lazoski C. Genetic homogeneity and historical expansions of the slipper lobster, *Scyllarides brasiliensis*, in the south-west Atlantic. *Mar Freshw Res*. 2014; 65: 59–69.
79. De Souza A, Júnior EAD, Galetti PM, Machado EG, Pichorim M, Molina WF. Wide-range genetic connectivity of Coney, *Cephalopholis fulva* (Epinephelidae), through oceanic islands and continental Brazilian coast. *An Acad Bras Cienc*. 2015; 87: 121–136. doi: [10.1590/0001-3765201520130411](https://doi.org/10.1590/0001-3765201520130411) PMID: [25806980](https://pubmed.ncbi.nlm.nih.gov/25806980/)
80. Hauser L, Carvalho GR. Paradigm shifts in marine fisheries genetics: ugly hypotheses slain by beautiful facts. *Fish and Fisheries*. 2008; 333–362.
81. Carvalho GR, Hauser L. Advances in the molecular analysis of fish population structure *Advances in the molecular analysis of fish population structure*. *Ital J Zool*. 1998; 65: 21–33.
82. Horne JB, van Herwerden L. Long-term panmixia in a cosmopolitan Indo-Pacific coral reef fish and a nebulous genetic boundary with its broadly sympatric sister species. *J Evol Biol*. 2013; 26: 783–799. doi: [10.1111/jeb.12092](https://doi.org/10.1111/jeb.12092) PMID: [23305496](https://pubmed.ncbi.nlm.nih.gov/23305496/)
83. Pruett CL, Saillant E, Gold JR. Historical population demography of red snapper (*Lutjanus campechanus*) from the northern Gulf of Mexico based on analysis of sequences of mitochondrial DNA. *Mar Biol*. 2005; 147: 593–602.
84. Da Silva R, Veneza I, Sampaio I, Araripe J, Schneider H, Gomes G. High levels of genetic connectivity among populations of yellowtail snapper, *Ocyurus chrysurus* (Lutjanidae—Perciformes), in the Western South Atlantic revealed through multilocus analysis. *PLoS One*. 2015; doi: [10.1371/journal.pone.0122173](https://doi.org/10.1371/journal.pone.0122173) PMID: [25769032](https://pubmed.ncbi.nlm.nih.gov/25769032/)
85. Ray N, Currat M, Excoffier L. Intra-Deme Molecular Diversity in Spatially Expanding Populations. *Mol Biol Evol*. 2003; 20: 76–86. PMID: [12519909](https://pubmed.ncbi.nlm.nih.gov/12519909/)
86. Nielsen R. Molecular signatures of natural selection. *Annu Rev Genet*. 2005; 39: 197–218. PMID: [16285858](https://pubmed.ncbi.nlm.nih.gov/16285858/)
87. Fahey AL, Ricklefs RE, Dewoody JA. DNA-based approaches for evaluating historical demography in terrestrial vertebrates. *Biol J Linn Soc*. 2014; 112: 367–386.
88. Ptak SE, Przeworski M. Evidence for population growth in humans is confounded by fine-scale population structure. *Trends Genet*. 2002; 18: 559–563. PMID: [12414185](https://pubmed.ncbi.nlm.nih.gov/12414185/)
89. Fernández Iriarte PJ, Pía Alonso M, Sabadin DE, Arauz PA, Iudica CM. Phylogeography of weakfish *Cynoscion guatucupa* (Perciformes: Sciaenidae) from the southwestern Atlantic. *Sci Mar*. 2011; 75: 701–706.
90. Grant WS. Problems and cautions with sequence mismatch analysis and Bayesian skyline plots to infer historical demography. *J Hered*. 2015; 106: 333–346. doi: [10.1093/jhered/esv020](https://doi.org/10.1093/jhered/esv020) PMID: [25926628](https://pubmed.ncbi.nlm.nih.gov/25926628/)
91. Allcock AL, Strugnell JM. Southern Ocean diversity: new paradigms from molecular ecology. *Trends Ecol Evol*. 2012; 27: 520–528. doi: [10.1016/j.tree.2012.05.009](https://doi.org/10.1016/j.tree.2012.05.009) PMID: [22727016](https://pubmed.ncbi.nlm.nih.gov/22727016/)
92. Funk WC, Mckay JK, Hohenlohe PA, Allendorf FW. Harnessing genomics for delineating conservation units. *Trends Ecol Evol*. 2012; 27: 489–496. doi: [10.1016/j.tree.2012.05.012](https://doi.org/10.1016/j.tree.2012.05.012) PMID: [22727017](https://pubmed.ncbi.nlm.nih.gov/22727017/)
93. Dawson MN, Barber PH, González-Guzmán LI, Toonen RJ, Dugan JE, Grosberg RK. Phylogeography of *Emerita analoga* (Crustacea, Decapoda, Hippidae), an eastern Pacific Ocean sand crab with long-lived pelagic larvae. *J Biogeogr*. 2011; 38: 1600–1612.